Original Article

Erythropoietin Enhances Endogenous CD34+ Stem Cells Mobilization and Inhibits Caspase-3 Mediated Apoptosis in the Cardiac Muscle of Doxorubicin Treated Rats: Histological Study

Noura H. Zidane[1], Nawal A. Hasanin[1], Zeinab A. Sakkara[1], Wafaa S. Hamed[1] and Amany A. AbdElfattah[1,2]

[1]*Department of Medical Histology & Cell Biology, Faculty of Medicine, Mansoura University, Mansoura, Egypt*

[2]*Department of Basic Medical Sciences, Faculty of Medicine, King Salman International University, South Sinai, Egypt*

ABSTRACT

Introduction: The use of Doxorubicin (DOX) as an antineoplastic drug is limited by its cardiotoxicity. Erythropoietin (EPO) has been suggested to be a powerful cardioprotective agent.

Aim of the Work: This study aimed to evaluate the protective role of EPO in DOX-induced cardiotoxicity and its role in mobilization of bone marrow-derived stem cells to the injured tissue.

Materials and methods: Thirty-two adult male albino rats (180-200 gm) were divided into equal four groups: control group (Gp I) received physiological saline (1 ml/kg/day), EPO group (Gp II) received recombinant human erythropoietin (rhEPO) (2500 IU/kg, 3 times a week), DOX-treated group (Gp III) received DOX (2.5 mg /kg, 3 times a week), DOX+EPO group (Gp IV) received DOX and rhEPO concomitantly. All medications were given by intraperitoneal injection for two weeks. Specimens from the left ventricles of all rats were prepared and stained for light microscopic study (hematoxylin & eosin, Masson's trichrome and phospho-tungstic acid hematoxylin in addition to immunohistochemical staining for caspase-3 and CD34) and transmission electron microscopic study.

Results: DOX caused marked alteration in the histological features of the cardiac muscle fibers as well as a highly significant increase in area percentage of the collagenous fibers and caspase-3 immunoexpression. Co-administration of EPO with DOX caused improvement in the histological features of the cardiac muscle fibers, a highly significant decrease in area percentage of the collagenous fibers and caspase-3 immunoexpression, and a highly significant increase in CD34 immunoexpression.

Conclusion: EPO exerts cardioprotective effects on DOX-induced cardiomyopathy via anti-apoptotic and anti-fibrotic pathways as well as via mobilization of stem cells to the injured tissues.

Received: 22 September 2022, **Accepted:** 20 October 2022

Key Words: Cardiotoxicity; caspase-3; CD34; doxorubicin; erythropoietin.

Corresponding Author: Noura H. Zidane, PhD, Department of Medical Histology & Cell Biology, Faculty of Medicine, Mansoura University, Mansoura, Egypt, **Tel.**: +20 10 0254 4204, **E-mail:** nourahassanzidan@gmail.com

ISSN: 1110-0559, Vol. 46, No. 4

INTRODUCTION

Doxorubicin (DOX), an anthracycline drug, is a commonly used chemotherapeutic agent for various malignancies[1]. After topoisomerase II complex has split the DNA chain for replication, DOX causes the complex to stabilize, which prevents the release of DNA double helix and stops replication. Additionally, DOX can boost the generation of quinone-type free radicals, therefore, contributing to its cytotoxicity[2].

The heart is highly sensitive to DOX poisoning with a particular concern in children with cancer, where DOX-associated cardiomyopathy can emerge many years following therapy[3,4].

DOX-induced cardiotoxicity is permanent and cumulative. It is the principal cause of mortality in DOX-treated patients[5]; therefore, research has been done to reduce DOX-induced cardiotoxicity by controlling apoptotic genes and oxidative stress[6].

Erythropoietin (EPO) is a glycoprotein hormone secreted in adults, mostly by the kidney and to a less extent by the liver, the vascular pericytes as well as the brain tissue[7]. EPO binds to its specific membrane receptor and prevents apoptosis of erythroid progenitor cells, hence regulates production of red blood cell in response to hypoxia[8]. EPO receptors existed in non-hematopoietic tissues, such as the heart and other organs that could rationalize extra-erythropoietic effects of EPO[9].

Exogenous EPO, recombinant human erythropoietin (rhEPO) is prepared by recombinant DNA technology and used to treat anemia in myelodysplasia, anemia in chronic kidney disease and anemia from cancer chemotherapy[10].

Personal non-commercial use only. EJH copyright © 2023. All rights served *DOI: 10.21608/ejh.2022.162368.1772*

Previous studies have revealed that EPO has multiple protective antioxidant, anti-inflammatory, and anti-apoptotic effects[11].

Endothelial progenitor cells (EPCs), hematopoietic stem cells (HSCs) and vascular endothelial cells all express the CD34 antigen (HSCs)[12]. In-depth research has focused on CD34+ cells, which are believed to have paracrine effects and the capacity to transdifferentiate, fuse with irreversibly damaged myocytes, and develop into endothelial cells[13].

Considering the restriction of DOX use as a chemotherapeutic drug due to its cardiotoxicity, the present study was designed to evaluate the role of EPO in amelioration and/or prevention of the changes that may occur in the cardiac muscle of adult male albino rats treated with DOX.

MATERIALS AND METHODS

Chemicals

A. Drugs

- Doxorubicin: Its trade name is Adribalstina, purchased from Pharmacia Italia S.P.A, Italy and available in the form of vials 50mg.
- Recombinant human erythropoietin: Its trade name is Epiao, purchased from Egyptian Pharmex Company and available in the form of vials 10,000 IU/l ml.

B. Kits

- Anti-caspase-3 polyclonal antibody (Catalogue number: ab4051, Abcam, Cambridge, United Kingdom).
- Anti-CD34 monoclonal antibody (Catalogue number: M 2165, Dako, Carpinteria, California, USA).

Experimental animals

Approval of the study was provided from Institutional Research Board (IRB), Faculty of Medicine, Mansoura University, with code: MD.19.07.203. Thirty-two adult male albino rats, two months old, weighing 180-200 gm, were obtained from Medical Experimental Research Center (MERC), Mansoura University and housed with regular day light/dark cycles and under adequate environmental conditions of temperature and ventilation. All rats received a standard rodent pellet diet and had free access to water. The rats were left for 2 weeks before starting the experiment to acclimatize to the room conditions and minimize nonspecific stress during the experiment.

Experimental design

Rats were randomly divided into four groups (8 rats for each group); Group I (control group): received physiological saline 1 ml/kg/day[14]. Group II (EPO group): received rhEPO dissolved in physiological saline (2500 IU/kg three times a week)[15]. Group III (DOX-treated group): received DOX (2.5 mg /kg three times a week, a cumulative dose of 15 mg/kg in 6 injections)[16]. Group IV (DOX+EPO group): received DOX and rhEPO (in the same mentioned doses above) concomitantly. All medications were given by intraperitoneal injection for two weeks.

Sampling and tissue processing

By the end of the 2nd week, all rats were injected intraperitoneally by sodium pentobarbital (40 mg/kg body weight) to be euthanized[17]. The heart of each rat was exposed by midline incision in the chest and the left ventricle was removed and processed for light and transmission electron microscopic studies.

Light microscopic study

Specimens of the left ventricles were immediately fixed in 10% formol saline, dehydrated and cleared then embedded in paraffin. Finally, serial sections at 5 µm thicknesses were obtained using a microtome and stained with hematoxylin & eosin stain (H&E)[18] for routine histological examination, Masson's trichrome stain[19] for identification of collagen fibers, phospho-tungstic acid hematoxylin (PTAH)[18] for demonstration of muscle striations and immunohistochemically for caspase-3 (marker of apoptosis) and CD34 (marker of endogenous stem cells)[20].

Immunohistochemistry staining procedures[20]

Specimens from the left ventricles were deparaffinized and rehydrated. Then, sections were microwaved for 15 minutes for antigen retrieval. After that, sections were treated with a blocking solution for 20 min then incubation with the primary rabbit polyclonal antibody for caspase-3 (at a dilution of 1:1000) and the primary mouse monoclonal antibody for CD34 (at a dilution of 1:40) at room temperature for 120 min. Later, secondary antibody was added for 10 minutes. Finally, one to two drops of DAB (diaminobenzidine) were added for 10 minutes. At last, the sections were counterstained with Mayer's hematoxylin, then dehydrated and cleared. Some slides were stained only with IgG secondary antibody and used as negative controls. Slides from human palatine tonsil and thymus were used as positive controls for caspase-3 and CD34 respectively.

Transmission electron microscopic study[21]

Tiny pieces (1 mm3) of the left ventricles were directly fixed overnight in 2.5% glutaraldehyde with 2% paraformaldehyde in a 0.1 M phosphate buffer (pH 7.4), and then fixed in 1 % of osmium tetroxide using the same buffer for 2 hours at 4°C. The tissue was then dehydrated and embedded in epoxy resin. Ultrathin sections were obtained and stained with uranyl acetate and lead citrate to be analyzed and captured using a transmission electron microscope (JEOL, JEM-2100, Tokyo, Japan) at the Faculty of Science, Alexandria University, Alexandria, Egypt.

Morphometric study

Slides were photographed with an Olympus E420 digital camera from China mounted on an Olympus microscope with a 0.5 × photo adaptor and a 40 × objective lens (TX31 Philippines). Following that, the images were examined by ImageJ 1.52a program (National Institutes of Health, United States) for assessment of area percentage of the collagenous fibers and immunoexpression. Area percentage of blue-stained collagenous fibers as well as area percentage of caspase-3 and CD34 immunoexpression were estimated in six non-overlapping fields/ section (6 sections from 6 different rats/ group) from Masson's trichrome, anti-caspase-3 and anti-CD34-stained sections, respectively.

Statistical analysis

The data achieved from the image analyzer were subjected to Statistical Package for Social Science version 22.0 (SPSS Inc., Chicago, USA). Statistical analysis using analysis of variance (ANOVA) followed by post hoc Tukey test was done. Data of all groups were expressed as mean ± standard deviation (± SD). Differences were regarded as significant if *P* (probability) value < 0.05 and highly significant if *P value* < 0.001[22].

RESULTS

Light Microscopic Results

H&E results

The control group (Figure 1) and EPO group (Figure 2) revealed the normal histological appearance of the myocardium. The cardiac muscle fibers were arranged in various directions (longitudinal, transverse, and oblique) (Figure 1a). The longitudinally cut cardiac muscle fibers were branching and anastomosing. Cardiac myocytes showed acidophilic faintly striated sarcoplasm and central oval vesicular nuclei with perinuclear spaces. Some cardiac myocytes were binucleated. Acidophilic intercalated discs (ICDs) between cardiac myocytes were also detected. The cardiac myocytes were surrounded by thin connective tissue layer (the endomysium) showing flattened darkly stained nuclei of fibroblasts (Figures 1 b,c , 2 a,b).

In DOX-treated group (Figure 3), the cardiac muscle fibers appeared disorganized and congested blood vessels were seen between the fibers (Figure 3a). Most of the longitudinally cut cardiac muscle fibers were corrugated with irregular and darkly stained pyknotic nuclei occupying variable positions. Other fibers were destructed. Vacuolated sarcoplasm, massive mononuclear cell infiltration and extravasation of blood cells were also seen (Figures 3 b,c,d).

The DOX+EPO group (Figure 4) showed restoration of the normal architecture of the cardiac muscle fibers apart from small areas of myofibrillar lysis, vacuolated sarcoplasm, and mononuclear cell infiltration.

Masson's trichrome stain results

Thin, blue-stained collagenous fibers of the endomysium were found among the cardiac muscle fibers in both control group (Figure 5a) and EPO group (Figure 5b). In DOX-treated group (Figure 5c), extensive deposition of collagenous fibers was seen among the muscle fibers. On the other hand, the DOX+EPO group showed less amount of collagenous fibers (Figure 5d).

PTAH stain results

The cross-banding pattern (striations) of the longitudinally cut cardiac muscle fibers were clearly seen in control group (Figure 6a) and EPO group (Figure 6b), while in DOX-treated group (Figure 6c), Most of the longitudinally cut cardiac muscle fibers lost their striations. Extravasated blood cells were also seen. The DOX+EPO group (Figure 6d) showed restoration of the cross-banding pattern of the cardiac muscle fibers.

Immunohistochemical results

Caspase-3 immune reaction

Immunohistochemical stained sections for caspase-3 showed negative immune reaction in the cardiomyocytes of both control group (Figure 7a) and EPO group (Figure 7b). A strong positive cytoplasmic and nuclear reaction was seen in most cardiac muscle fibers in DOX-treated group (Figure 7c), however, few cells with positive immune reaction were found in the DOX+EPO group (Figure 7d).

CD34 immune reaction

Immunohistochemical stained sections for CD34 showed positive immune reaction in the endogenous stem cells among the cardiac muscle fibers and in the endothelial layer of the blood vessels in both control group (Figure 8a) and EPO group (Figure 8b), apparent increase in DOX-treated group (Figure 8c) and more increase in DOX+EPO group (Figure 8d).

Electron microscopic results

The control group (Figure 9 a,b,c,d) and the EPO group (Figure 10 a,b,c) showed similar histological appearance. The cardiac muscle fibers showed regularly arranged myofibrils with well-organized sarcomeres extending between the Z lines with alternating dark (A) and light (I) bands intersected by H zones and Z lines, respectively. A central oval euchromatic nuclei were seen. Intermyofibrillar mitochondria (IMFM) with abundant tubular cristae were packed in longitudinal rows between the myofibrils. Perinuclear mitochondria (PNM) were seen at the poles of the nuclei and appeared more rounded and smaller compared to the complex shaped and larger IMFM. The sarcoplasmic reticulum (SR) appeared between two mitochondria and at the Z line of the sarcomere. A characteristic step-like ICDs with prominent adherens junctions and desmosomes in the transverse parts as well as gap junctions in the longitudinal parts were seen.

The DOX-treated group (Figure 11 a,b,c,d) showed disruption and fragmentation of the myofibrils, disorganized sarcomeres as well as less defined and disrupted Z lines. Some Z lines appeared thickened. Areas of myofibrillar lysis were seen. IMFM were swollen with abnormal shapes and irregular distribution between the disorganized myofibrils. Most nuclei of the cardiomyocytes were shrunken and had corrugated envelopes as well as condensed heterochromatin. PNM were disrupted and wide areas of empty spaces appeared around the nuclei. There were widening and disruption in the ICDs as well as multiple vacuoles and areas of SR dilatation.

Cardiomyocytes from DOX+EPO group (Figure 12 a,b,c) showed normal ultrastructural appearance apart from small areas of destructed myofibrils and some disrupted IMFM.

Image analysis results and statistical analysis

The mean area percentage of the collagenous fibers showed non-significant change ($p > 0.05$) in EPO group, compared to the control group, and showed a high significant increase ($P < 0.001$) in DOX treated group versus control and EPO groups. However, DOX+EPO group showed a high significant reduction ($P < 0.001$) compared to DOX-treated group and non-significant increase ($P > 0.05$) compared to control and EPO groups (Table 1, Histogram 1).

The mean area percentage of caspase-3 immunoexpression showed non-significant change ($P > 0.05$) in EPO group compared to the control group and showed a high significant increase ($P < 0.001$) in DOX treated group versus control and EPO groups. However, DOX+EPO group showed a high significant reduction ($P < 0.001$) compared to DOX treated group, significant increase ($P < 0.05$) compared to control group and non-significant increase ($P > 0.05$) compared to EPO group (Table 2, Histogram 2).

The mean area percentage of CD34 immunoexpression showed a significant increase ($P < 0.05$) in EPO group compared to the control group while DOX treated group showed a high significant increase ($P < 0.001$) compared to the control group and a non-significant increase ($P > 0.05$) compared to EPO group. DOX+EPO group showed a high significant increase ($P < 0.001$) in the mean area percentage of CD34 immunoexpression compared with that of the control, EPO and DOX treated groups (Table 2, Histogram 3).

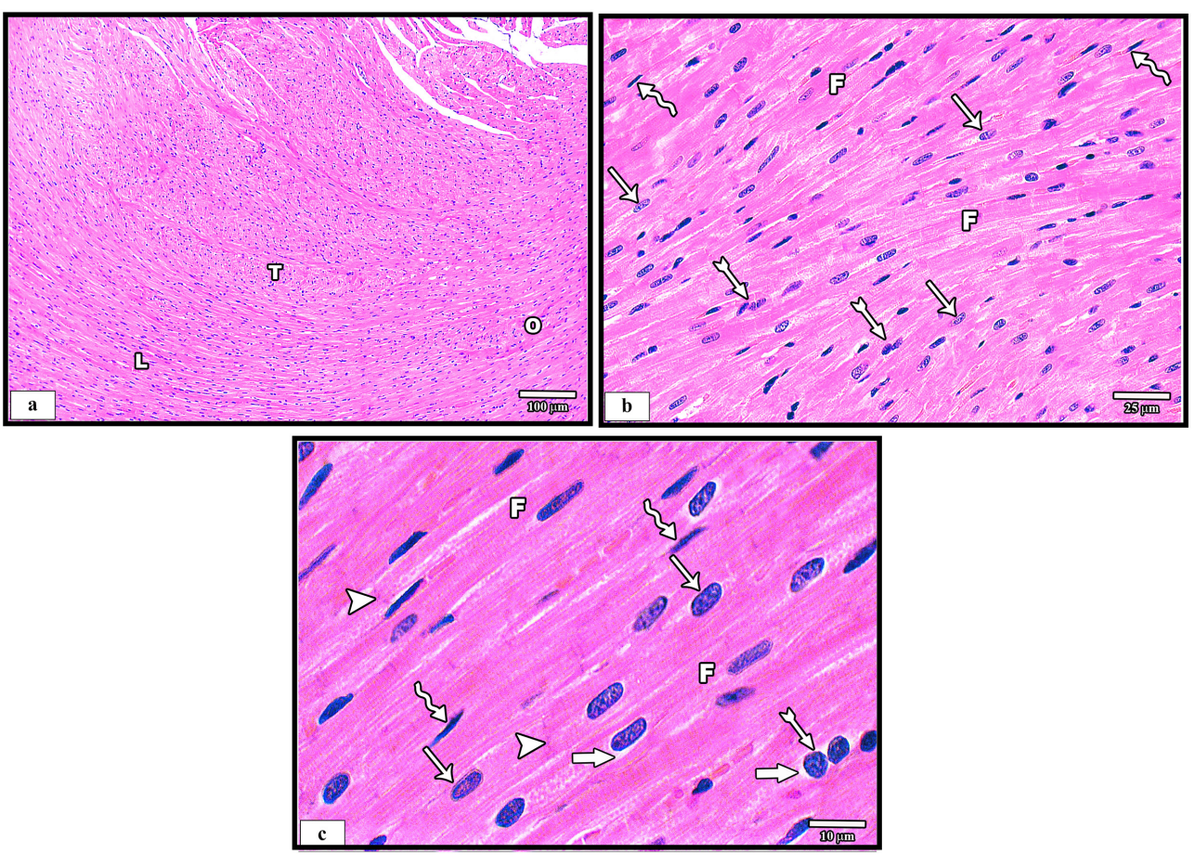

Fig. 1: H&E-stained section in the myocardium of the left ventricle of control group (Gp I).

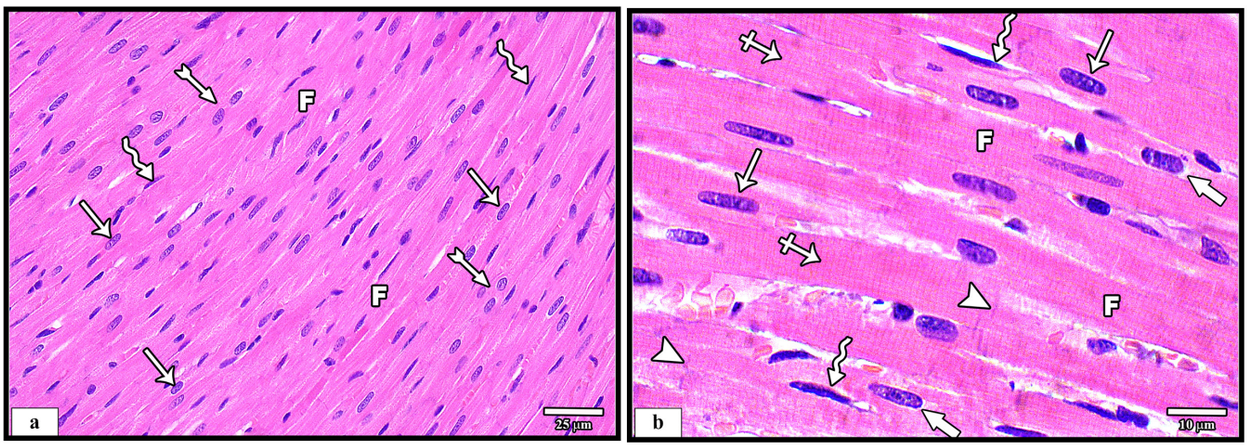

Fig. 2: H&E-stained section in the myocardium of the left ventricle of EPO group (Gp II) showing longitudinally cut cardiac muscle fibers (F) which are branching and anastomosing and have acidophilic sarcoplasm and vesicular oval centrally located nuclei (arrows). The fibers show fine irregular transverse striations (crossed arrows) and acidophilic ICDs (arrowheads). Delicate connective tissue (the endomysium) containing fibroblasts with flattened darkly stained nuclei (zigzag arrows) are seen between the fibers. Notice the presence of perinuclear spaces (thick arrows) in some fibers (a ×400; b ×1000)

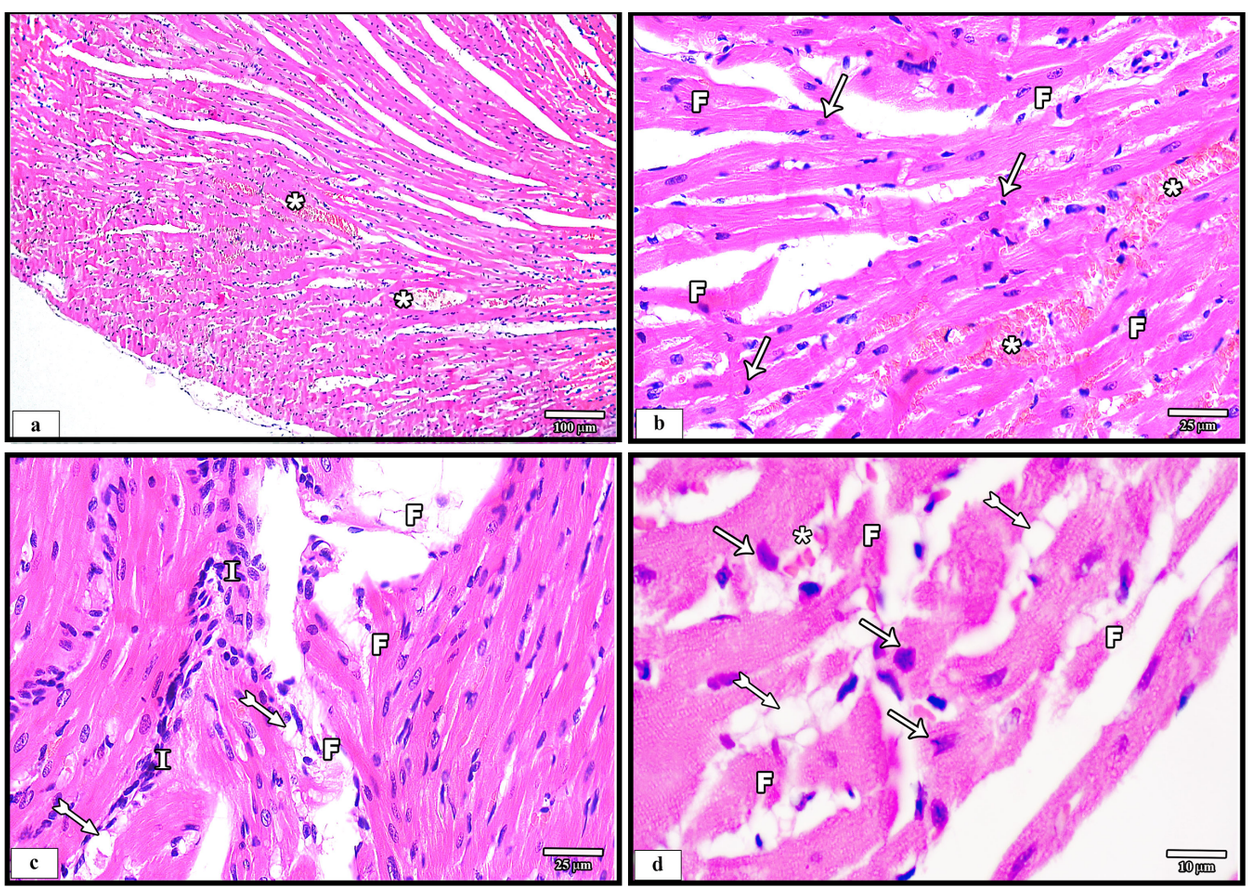

Fig. 3: H&E-stained section in the myocardium of the left ventricle of DOX treated group (Gp III). (a) showing disorganized cardiac muscle fibers with congested blood vessels (*) in-between. (b) showing longitudinally cut corrugated muscle fibers (F) with loss of normal orientation and continuity. The nuclei (arrows) appear irregular, pyknotic and occupy variable positions. Extravasated blood cells (*) are seen between the fibers. (c) showing markedly disrupted cardiac muscle fibers (F). Vacuolated sarcoplasm (forked arrows) of some cardiomyocytes and massive mononuclear cell infiltration (I) are also seen (d) showing destruction in some fibers (F) and extravasated blood (*) in-between. The nuclei (arrows) of the fibers appear irregular, pyknotic and of variable positions. Vacuolated sarcoplasm (forked arrows) appears in some fibers (a ×100; b & c ×400; d ×1000)

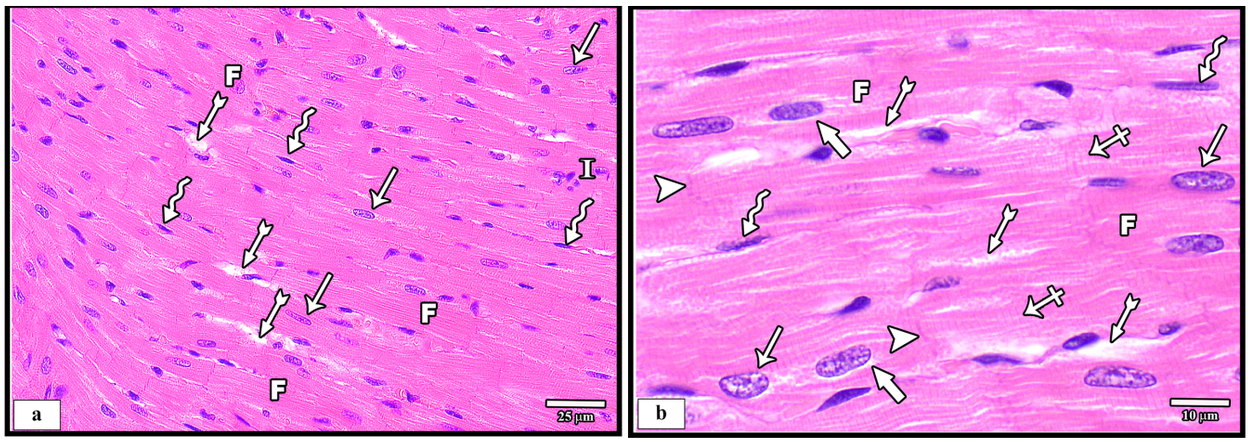

Fig. 4: H&E-stained section in the myocardium of the left ventricle of DOX+EPO group (Gp IV). (a & b) showing longitudinally cut cardiac muscle fibers with restoration of the normal architecture. The fibers (F) are branching and anastomosing with acidophilic sarcoplasm and vesicular oval centrally located nuclei (arrows). Perinuclear spaces (thick arrows) appear in some fibers. The fibers show fine irregular transverse striations (crossed arrows) and acidophilic ICDs (arrowheads). Delicate connective tissue containing fibroblasts with flattened darkly stained nuclei (zigzag arrows) are seen between the fibers. Few fibers with vacuolated sarcoplasm and areas of myofibrillar lysis (forked arrows) are seen. A small area of mononuclear cell infiltration (I) is also seen (a ×400; b ×1000)

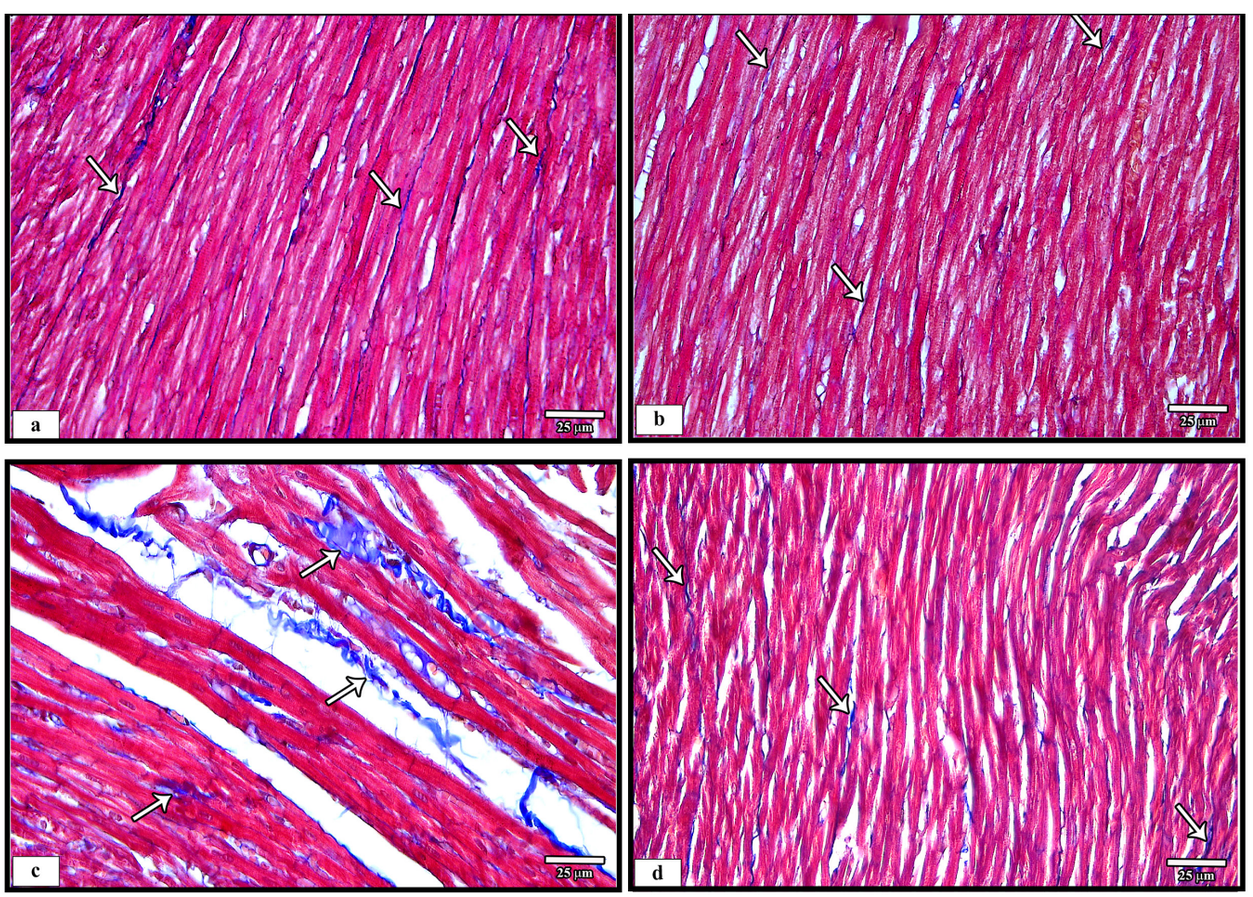

Fig. 5: Masson's trichrome stained sections in the myocardium of the left ventricle among the different groups. (a) control group (Gp I) and (b) EPO group (Gp II) showing thin blue-stained collagenous fibers (arrows) in the endomysium among the longitudinally cut cardiac muscle fibers. (c) DOX treated group (Gp III) showing extensive deposition of blue-stained collagenous fibers (arrows). Compare with control group (a). (d) DOX+EPO group (Gp IV) showing less blue-stained collagenous fibers deposition (arrows). Compare with DOX treated group (c) (×400)

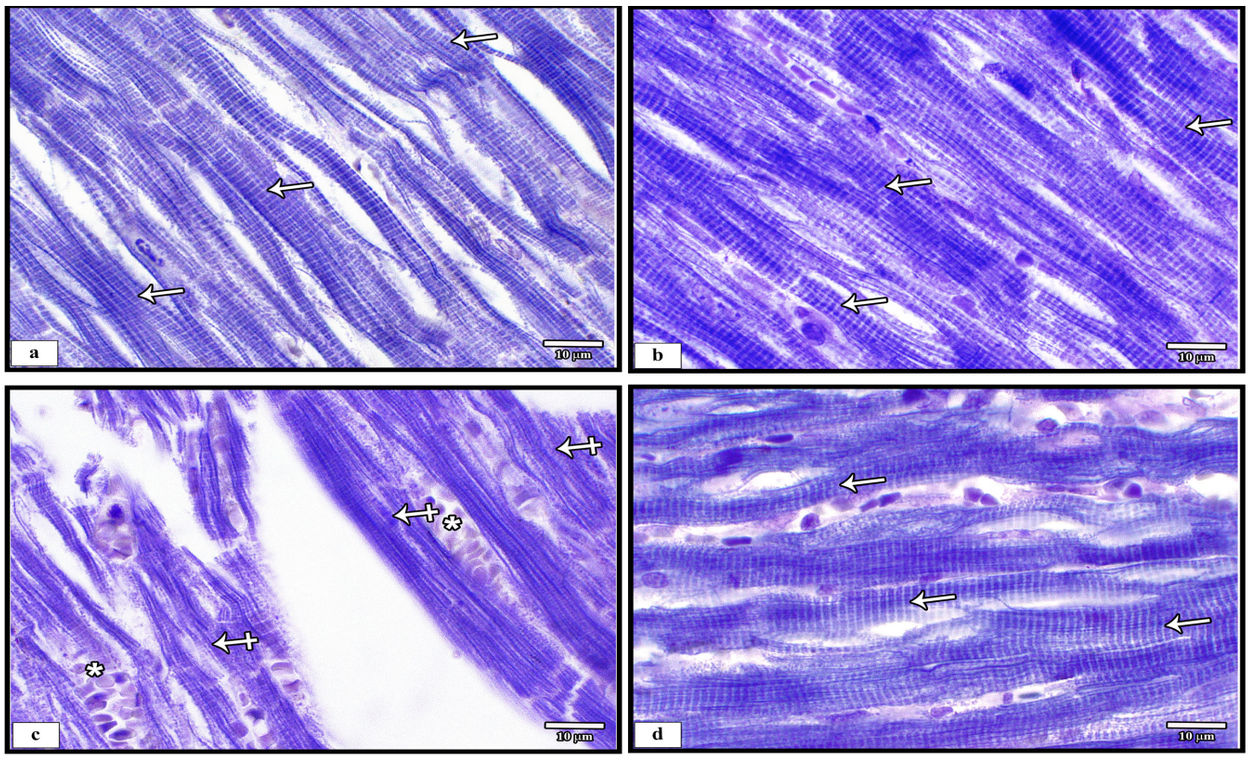

Fig. 6: PTAH stained sections in the myocardium of the left ventricle among the different groups. (a) control group (Gp I) and (b) EPO group (Gp II) showing evident transverse striations (arrows) along the longitudinally cut cardiac muscle fibers. (c) DOX treated group (Gp III) showing loss of striations (crossed arrows) in the majority of the fibers. Extravasated blood cells (*) between the cardiac muscle fibers are also seen. (d) DOX+EPO group (Gp IV) showing restoration of the striations (arrows) of the fibers (×1000)

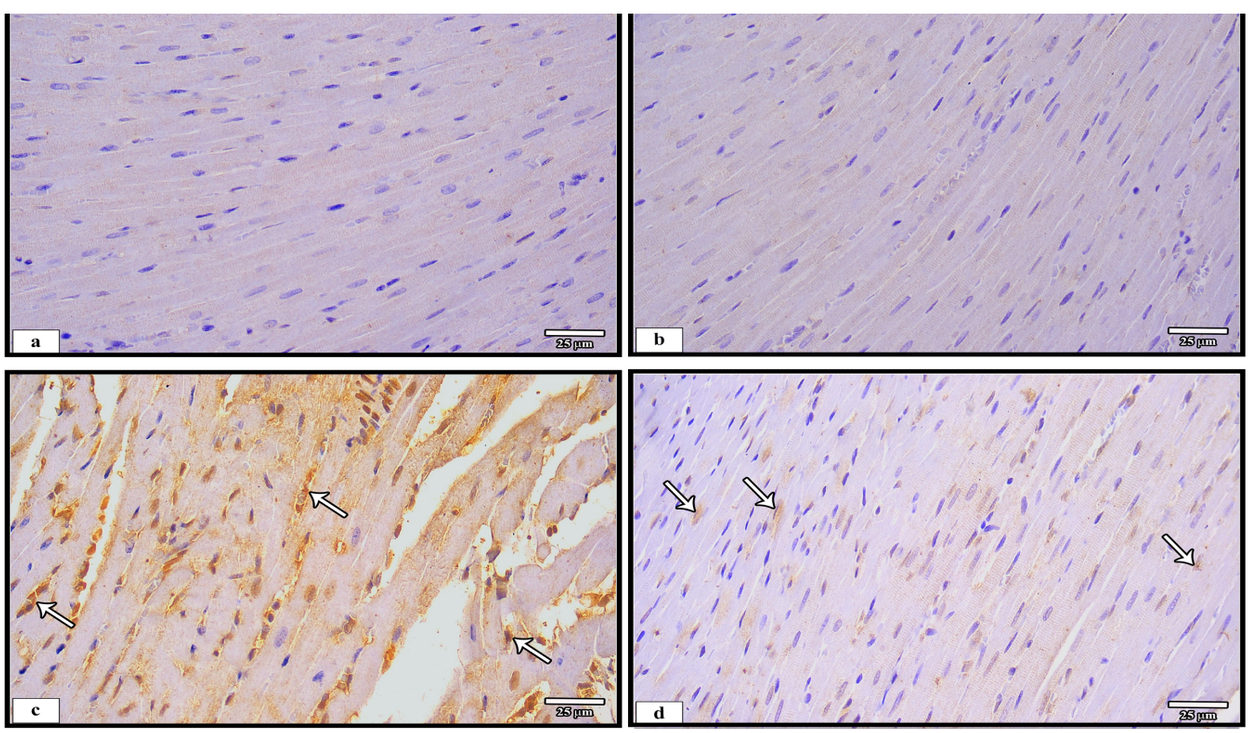

Fig. 7: Caspase-3 immuno-stained sections in the myocardium of the left ventricle of different groups showing longitudinally cut cardiac muscle fibers. (a) control group (Gp I) and (b) EPO group (Gp II) showing negative caspase-3 immune reaction. (c) DOX treated group (Gp III) showing obvious positive caspase-3 immune reaction (arrows) (d) DOX+EPO group (Gp IV) showing minimal positive caspase-3 immune reaction (arrows) (×400)

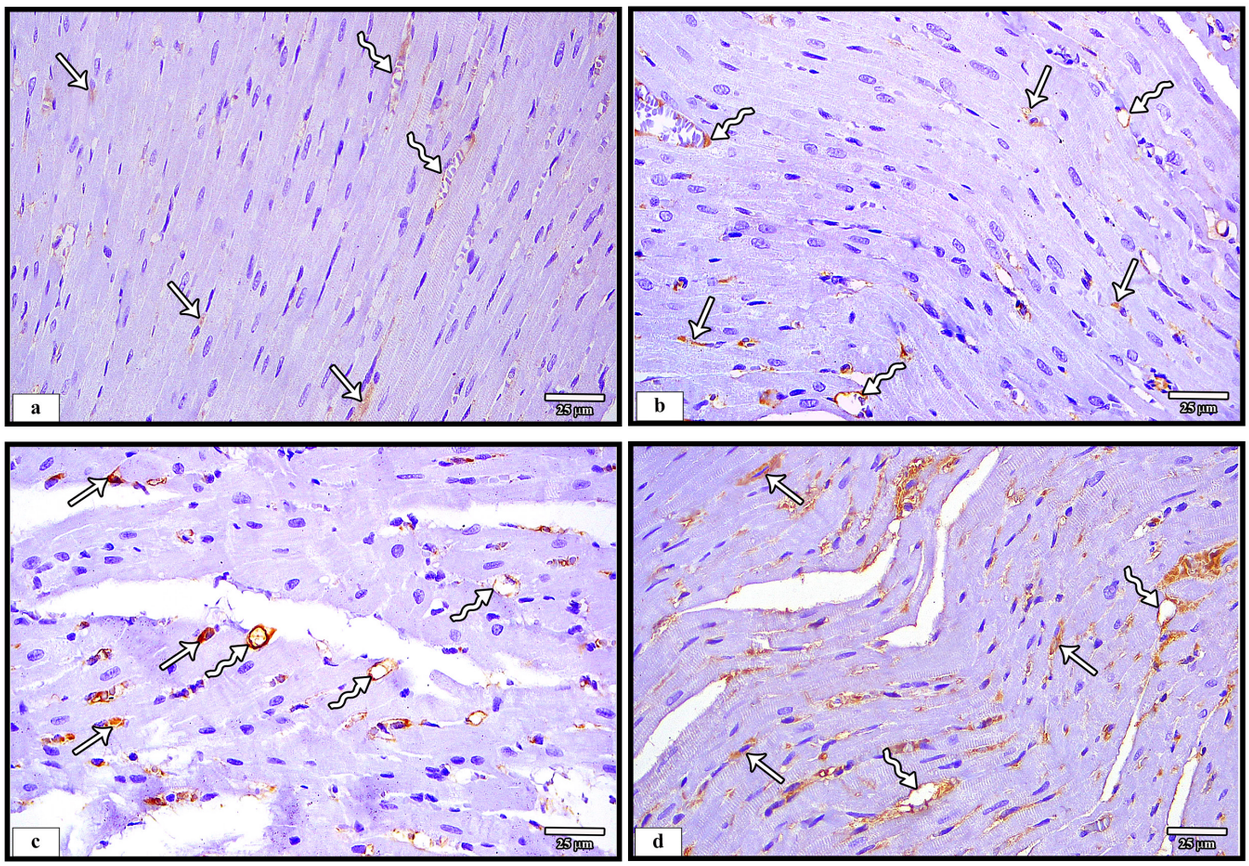

Fig. 8: CD34 immuno-stained sections in the myocardium of the left ventricle of different groups showing positive immune reaction in the endogenous stem cells (arrows) among the cardiac muscle fibers and in the endothelial lining of the blood vessels (zigzag arrows). (a) control group (Gp I) showing few positive immune reactions. (b) EPO group (Gp II) showing more positive immune reaction than control group. (c) DOX treated group (Gp III) showing obvious positive immune reaction more than control and EPO group. (d) DOX+EPO group (Gp IV) showing apparent increase in positive immune reaction compared with the other groups (×400)

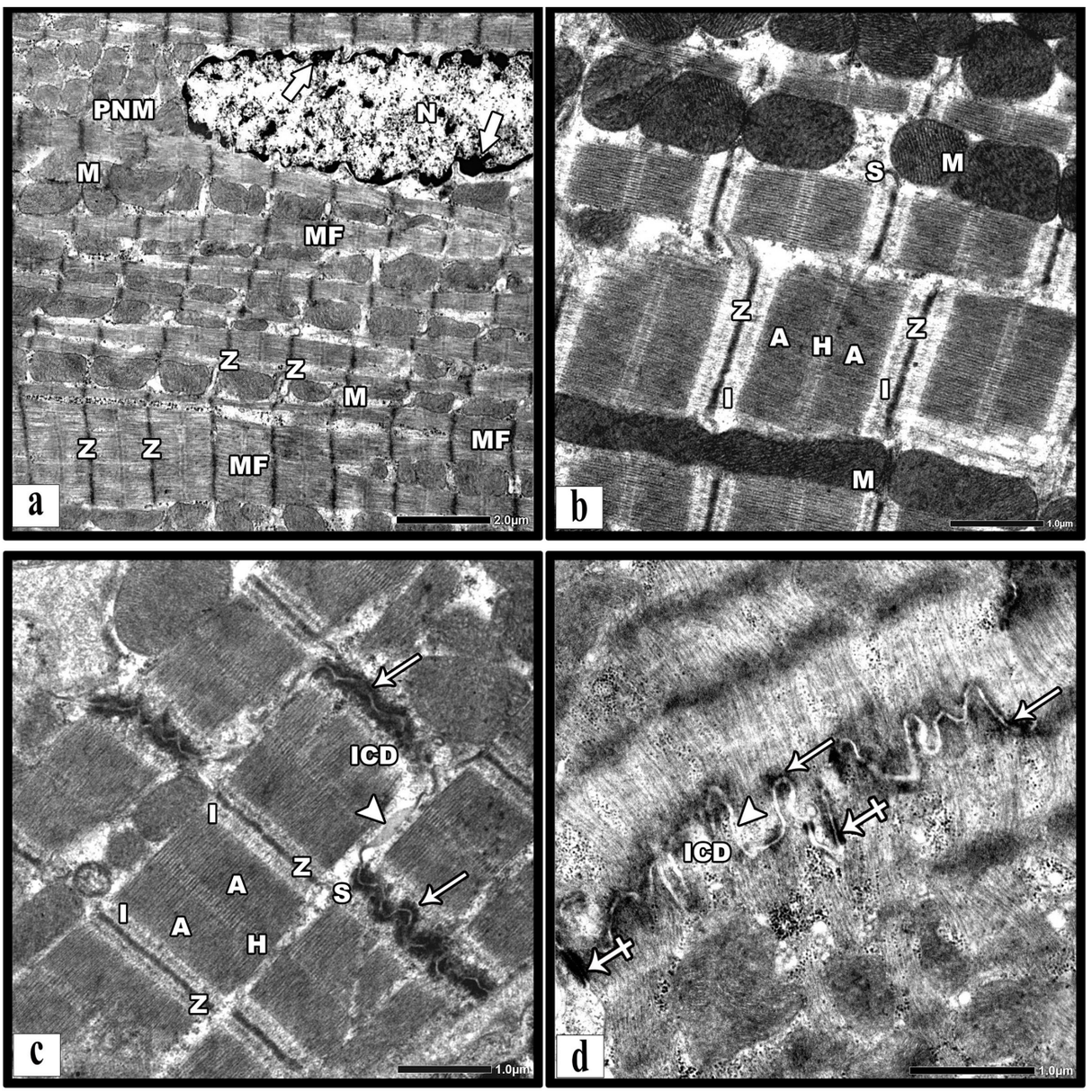

Fig. 9: Electron micrographs of the myocardium of the left ventricle of control group (Gp I) (a, b &c) showing regularly arranged myofibrils (MF) with well-organized sarcomeres extending between Z lines (Z). Intermyofibrillar mitochondria (M) are packed in longitudinal rows among the myofibrils. The nucleus (N) appears euchromatic with peripheral heterochromatin (thick arrows). Perinuclear mitochondria (PNM) are present at the pole of the nucleus and are more rounded and smaller compared to the complex-shaped and larger intermyofibrillar mitochondria. The sarcomere has dark (A) band, two halves of light (I) bands and H zone (H). The sarcoplasmic reticulum (S) sits between two mitochondria and at the Z line of the sarcomere. (c & d) showing zigzag like intercalated disc (ICD) with prominent adherens junctions (arrows) as well as desmosomes (crossed arrows) in the transverse parts and gap junctions (arrowhead) in the longitudinal parts. (a ×12,500; b & c ×25,000; d ×35,000)

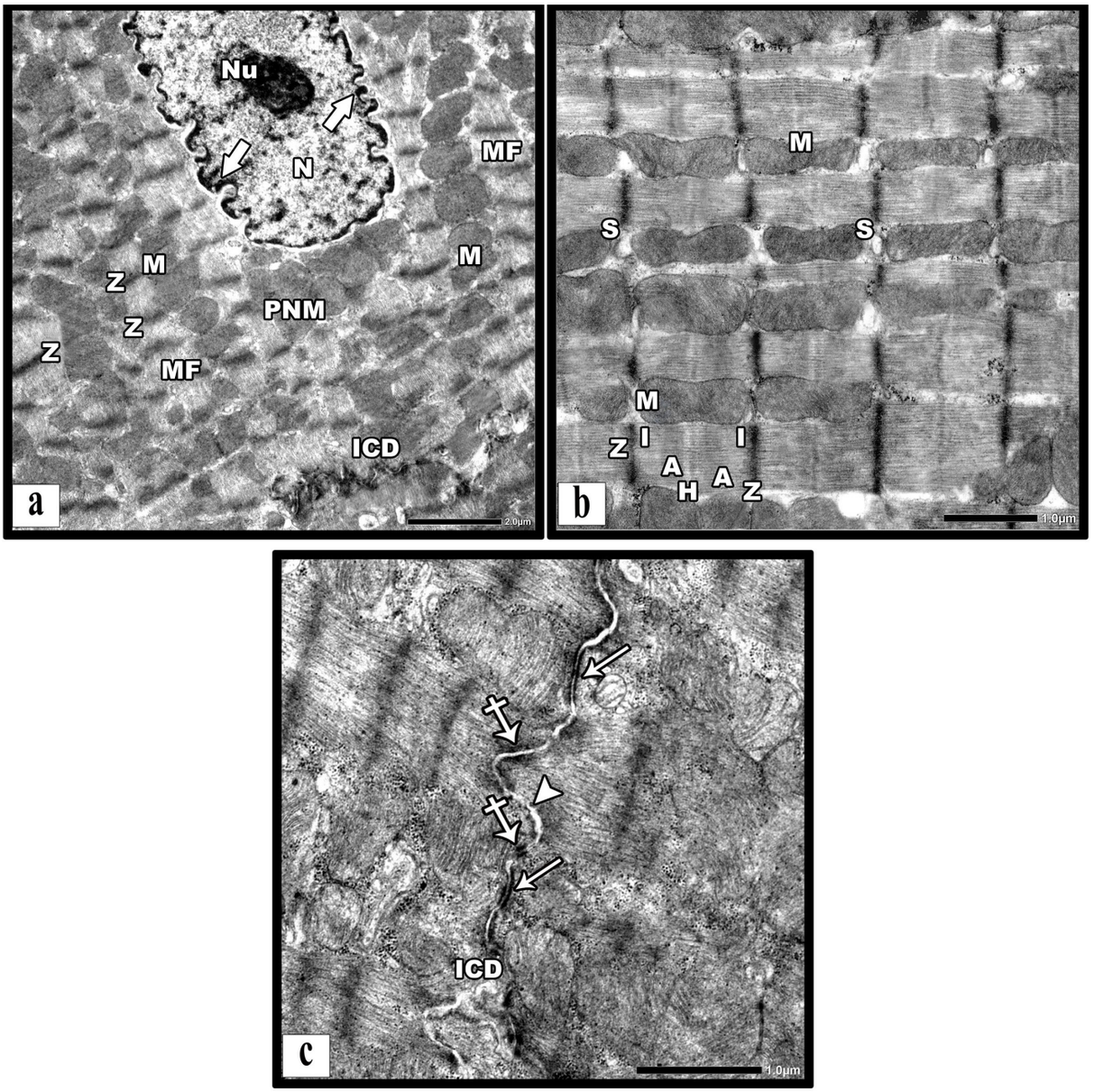

Fig. 10: Electron micrographs of the myocardium of the left ventricle of EPO group (Gp II) (a &b) showing regularly arranged myofibrils (MF) with well-organized sarcomeres extending between two Z lines (Z). Intermyofibrillar mitochondria (M) are packed in longitudinal rows among the myofibrils. The nucleus (N) appears euchromatic with peripheral heterochromatin (thick arrows) and prominent nucleolus (Nu). Perinuclear mitochondria (PNM) are seen at the pole of the nucleus. The sarcomere shows dark (A) band, two halves of light (I) bands and H zone (H). The sarcoplasmic reticulum (S) sits between two mitochondria and at the Z line of the sarcomere. (a&c) showing zigzag like intercalated disc (ICD) between two cardiac myocytes having prominent adherens junctions (arrows), desmosomes (crossed arrows) and gap junction (arrowhead). (a ×12,500; b ×25,000; c ×35,000)

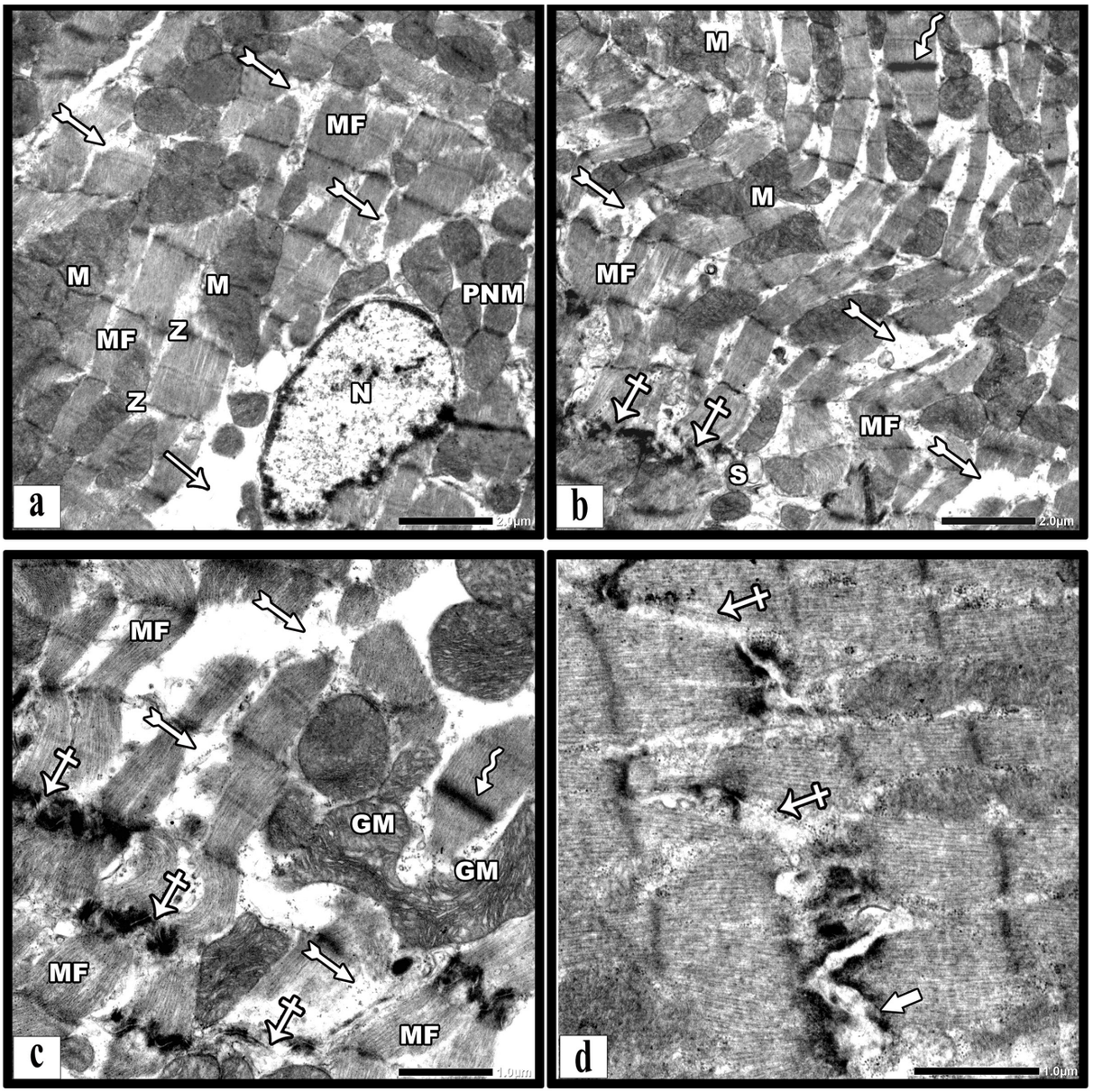

Fig. 11: Electron micrographs of the myocardium of the left ventricle of DOX treated group (Gp III). (a, b &c) showing disrupted myofibrils (MF) with disorganized sarcomeres extending between less defined and disrupted Z lines (Z). Some Z lines appear thickened (zigzag arrows). Areas of myofibrillar lysis (forked arrows) are seen. The nucleus (N) is shrunken with corrugated nuclear envelope and perinuclear empty space (arrow). Perinuclear mitochondria (PNM) are seen at one pole of the nucleus. Intermyofibrillar mitochondria (M) are swollen and distorted with irregular shape and distribution between myofibrils and some are giant (GM). (b) showing dilated tubules of the sarcoplasmic reticulum (S). (b, c &d) showing disruption (crossed arrows) and widening (thick arrow) of the ICD (a&b ×12,500; c ×25,000; d ×35,000)

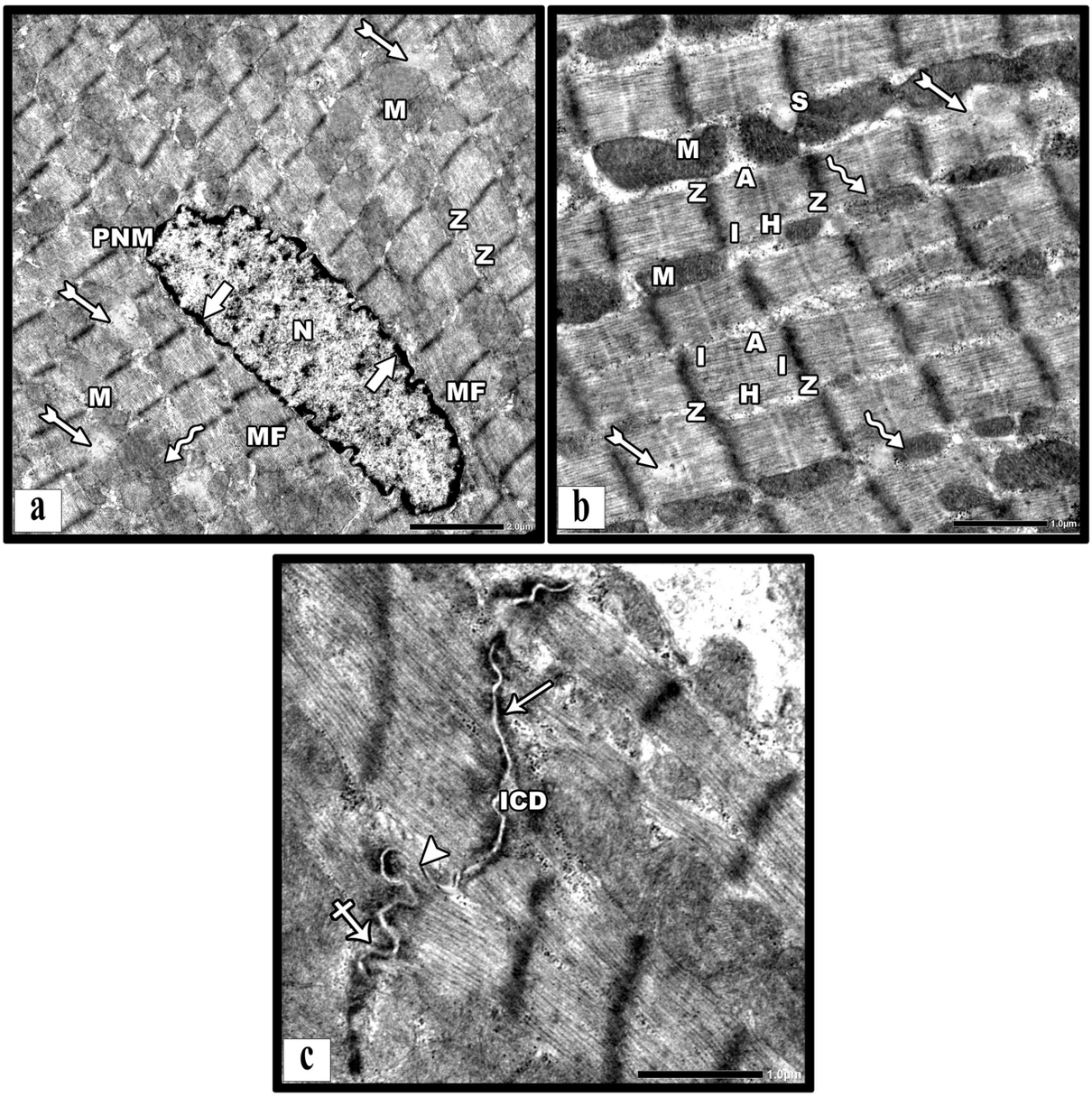

Fig. 12: Electron micrographs of the myocardium of the left ventricle of DOX+EPO group (Gp IV). (a, b &c) showing regularly arranged myofibrils (MF) with well-organized sarcomeres extending between two Z lines (Z). Intermyofibrillar mitochondria (M) packed in longitudinal rows among the myofibrils. The nucleus (N) appears euchromatic with peripheral heterochromatin (thick arrows). Perinuclear mitochondria (PNM) are seen at the pole of the nucleus. The sarcomere shows dark (A) band, two halves of light (I) bands and H zone (H). The sarcoplasmic reticulum (S) sits between two mitochondria and at the Z line of the sarcomere. Well-organized and apparently normal intercalated disc (ICD) having prominent adherens junction (arrow), desmosome (crossed arrow) and gap junction (arrowhead) is seen. (a&b) showing small areas of destructed myofibrils (forked arrows) and some disrupted intermyofibrillar mitochondria (zigzag arrows) (a ×12,500; b ×25,000; c ×35,000)

Table 1: Area percentage of the collagenous fibers between different groups (Mean ± SD)

Parameters	Control group (Gp I)	EPO group (Gp II)	DOX-treated group (Gp III)	DOX+EPO group (Gp IV)
Area % of collagenous fibers (Mean + SD)	2.63 ± 0.19	2.86 ± 0.13	11.49 ± 1.63	3.18 ± 1.06
		*P*1 = 0.975	*P*1 < 0.001**	*P*1 = 0.761
			*P*2 < 0.001**	*P*2 = 0.942
				*P*3 < 0.001**

SD= the standard deviation, *P*: Probability of ANOVA, *P*1: Significance versus Gp I, *P*2: Significance versus Gp II, *P*3: Significance versus Gp III, *: significance <0.05, **: high significance <0.001.

Table 2: Area percentage of positive caspase-3 and CD34 immune reaction between different groups (Mean ± SD)

Parameters	Control group (Gp I)	EPO group (Gp II)	DOX-treated group (Gp III)	DOX+EPO group (Gp IV)
Area % of positive caspase-3 immune reaction (Mean + SD)	0.32± 0.14	0.62 ± 0.27	17.28 ± 1.23	1.53 ± 0.13
		*P*1 = 0.857	*P*1 < 0.001**	*P*1 = 0.019*
			*P*2 < 0.001**	*P*2 = 0.096
				*P*3 < 0.001**
Area % of positive CD34 immune reaction (Mean + SD)	0.68 ± 0.095	1.41 ± 0.09	1.75 ± 0.12	7.31 ± 0.62
		*P*1 = 0.004*	*P*1 < 0.001**	*P*1 < 0.001**
			*P*2 < 0.305	*P*2 < 0.001**
				*P*3 < 0.001**

SD= the standard deviation, *P*: Probability of ANOVA, *P*1: Significance versus Gp I, *P*2: Significance versus Gp II, *P*3: Significance versus Gp III, *: significance <0.05, **: high significance <0.001.

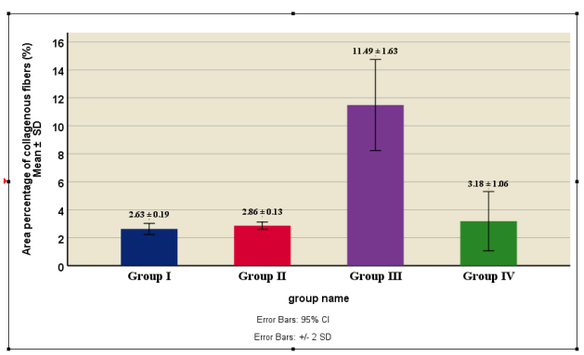

Histogram 1: Mean area percentage of collagenous fibers in different groups

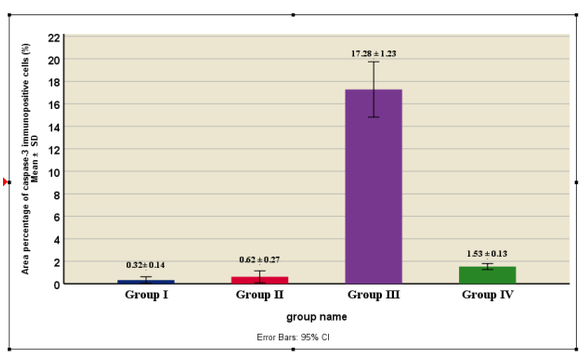

Histogram 2: Mean area percentage of positive caspase-3 immune reaction in different groups

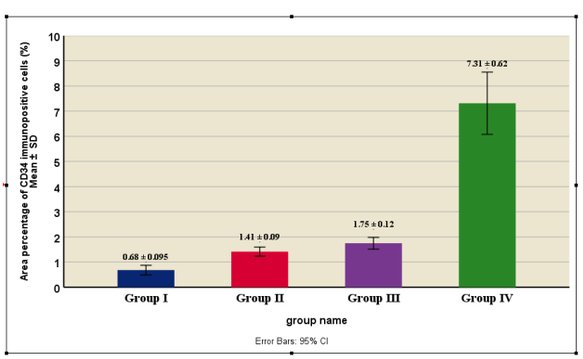

Histogram 3: Mean area percentage of positive CD34 immune reaction in different groups

DISCUSSION

Doxorubicin (DOX) is a commonly used chemotherapeutic drug and its clinical effect is well recognized. However, patients treated with DOX are at a high risk of cardiotoxicity. DOX-induced toxicity in cardiac myocytes have been attributed to several mechanisms including oxidative stress, mitochondrial disruption, metabolic derangements, and initiation of apoptotic cascade. Yet, effective prevention and treatment of DOX-induced cardiotoxicity did not emerge[23,24].

Erythropoietin, a glycoprotein hormone, reduces tissue hypoxia by increasing systemic oxygen-carrying capacity. It stimulates erythroid precursor cell proliferation and differentiation to compensate for the reduced oxygen levels caused by hypoxia and anemia. In models of cardiac, neuronal, retinal, and renal ischemia injury, EPO exhibits tissue-protective effects by a variety of mechanisms, including suppression of apoptosis, reduction of inflammation, neovascularization, and restoration of tissue function[25]. Therefore, the current study aimed to highlight the possible cardioprotective role of EPO on DOX-induced cardiomyopathy in a rat model with special emphasis on its anti-apoptotic role as well as its role in enhancing mobilization of bone marrow derived stem cells to the site of injury.

Light microscopic examination of both control and EPO groups revealed the normal histological appearance of the cardiac muscle fibers. On the other hand, there was disorganization of the cardiac muscle fibers in DOX-treated group with corrugation or destruction of the fibers, massive mononuclear cell infiltration and extensive deposition of collagenous fibers.

Reactive oxygen species (ROS) overproduction and cardiomyocyte apoptosis are two examples of the several variables that have been shown to have a role in the pathogenesis of DOX-induced cardiac damage. Overproduction of ROS disrupts cellular membrane integrity and function and causes oxidative damage to biological macromolecules. Furthermore, cardiomyocyte apoptosis can be directly caused by DOX-induced oxidative stress[26]. Previous studies also proved that DOX stimulates the expression of death receptors in normal cells including cardiomyocytes, resulting in apoptosis[4].

Additionally, DOX depletes GATA-4 a member of the zinc finger transcription factor. GATA-4 has a critical role in promoting cardiac development and myocardial differentiation as well as regulating the hypertrophic growth and survival of the heart[27].

A high significant increase in the mean area percentage of the collagenous fibers was detected among the cardiac muscle fibers of the DOX-treated group of our study compared to the control group. These results run with that published by Pajović *et al*. (2021); Goda *et al*. (2021) and Abdo *et al*. (2019)[23,28,29]. The later suggested that increase deposition of collagenous fibers might be due to increase in the activity of fibroblasts under the effect of free radical stress of DOX. On the other hand, a previous study by Rodrigues *et al*. (2019) showed that the increase in interstitial fibrosis in the early stages of DOX-induced cardiotoxicity is attributable to activation of the NF-κB transcription factor[30].

Obvious caspase-3 positive immune reaction among the cardiac myocytes was seen in the DOX-treated group and represented statistically by a highly significant increase in the mean area percentage compared to control and EPO groups. This result can be explained in light of the concept of Zhao and Zhang (2017) and Ye *et al*. (2022) who suggested that caspases are key molecules in the mechanisms of DOX-stimulated cardiomyocyte apoptosis[31,32]. Shati (2020) stated that DOX can induce cardiotoxicity through the formation of ROS promoting necrosis and apoptosis. This indicate the enhanced effect of caspase-3 activity as an important marker of apoptosis and these changes might be the result of increased oxidative stress associated with low antioxidant defenses, resulting in cellular and DNA damage consequently[33].

Focal areas of disruption, fragmentation or even lysis of some myofibrils at the ultrastructural level of DOX-treated group may be resulted from oxidative injury to the cardiac myocytes. Seke *et al*. (2019) and Jin *et al*. (2021) considered the myofibrillar injury observed in their studies as a secondary event after mitochondrial dysfunction. In the current study, the previous assumption is confirmed by the presence of significant mitochondrial morphological changes in the form of deformation, variability in size, swelling and lack of intact cristae[34,35]. The same findings were also observed by Yin *et al*. (2018) and Sergazy *et al*. (2020)[36,37]. On the other hand, disrupted and thickened Z lines seen in our study may be related to DOX interaction with actin filaments which are essential components of thin filaments and Z lines. The observed apparent thickened Z lines in some areas may be due to actin polymerization. However, disrupted Z lines appeared in other areas may be attributed to inhibition of protein synthesis and therefore decrease in the level of sarcoplasmic actin[38].

Deterioration and disorganization of ICDs were seen in DOX-treated group. The interdigitation of ICDs was disrupted throughout the tissue. Gap junctions in ICDs are thought to mediate the electrical connection between cardiac myocytes and maintain the regular heartbeat. Connexins are the building blocks of each gap junctional channel. Connexin43 (Cx43) is the most prevalent isoform of connexin in mammalian cardiac cells. Myocardial disorders include hypertrophic cardiomyopathy, ischemia, and heart failure are associated with changes in Cx43 distribution and expression[39].

Ito *et al*. (2021) and Li *et al*. (2021) added that dilated cardiomyopathy (DCM) can be induced by knockout of the N-cadherin gene and therefore it is considered as a disorder of the ICDs[40,41]. Moreover, in some DCM cases, germline mutations have been reported in genes coding for ICD-associated membrane proteins[42].

In the current study, EPO administration for two weeks in concomitant with DOX showed restoration of the normal cardiac muscle architecture at the level of both light and transmission electron microscope.

The protective impacts of EPO have been explained by a variety of different mechanisms. EPO has been proved to have antioxidant effect by promoting the production of the antioxidant enzyme heme oxygenase-1, which catalyzes the breakdown of heme to produce biliverdin, CO, and free iron, and reduces the creation of superoxide anion (O2-)[43]. EPO has been also proved to reduce ROS generation by inhibiting the activation of nicotinamide adenine dinucleotide phosphate hydrogen (NADPH) oxidase[44].

In our study, there was a high significant decrease in area percentage of caspase-3 positive immune reaction in DOX+EPO group as compared to DOX-treated group. EPO has been considered as an anti-apoptotic, tissue-protective cytokine. EPO protects neurons against apoptosis through increasing the expression of the antiapoptotic protein Bcl-2 and decrease the expression of the proapoptotic protein Bax[45]. This causes a decrease in the expression and release of key indicators of the intrinsic apoptotic pathway of mitochondria, including cytochrome c and caspase-3, the main executioner of the apoptotic pathway of mitochondria[46]. EPO has also been demonstrated to restore GATA-4 (a key regulator of cardiac development) expression in DOX-induced cardiomyopathy[9]. Furthermore, EPO restores the DOX-induced alterations in sarcomeric proteins, including troponin I, myosin heavy chain and desmin. These proteins maintain the structural integrity and contractile function of cardiomyocytes[47].

He *et al*. (2018) indicated that EPO exerts protective effects on lung injuries after lung ischemia/reperfusion injury through inhibiting the toll-like receptor-4/nuclear factor-κB (TLR4/NF-κB) signaling pathway and decreasing production of inflammatory cytokines (TNF-α, IL-6, and IL-1β)[48]. This may explain the anti-inflammatory effect of EPO in our study.

A high significant decrease in the mean area percentage of collagenous fibers among the cardiac muscle fibers was detected in DOX+EPO group compared with DOX-treated group. Our results run with that published by Lu *et al*. (2012) who found that administration of EPO in diabetic rat inhibited myocardial fibrosis by decrease the level of transforming growth factor beta (TGF-β) expression as well as decrease the deposition of interstitial collagen[49]. Additionally, administration of EPO in rats with myocardial fibrosis induced by pressure overload caused reduction in proliferation and differentiation of cardiac fibroblast as well as accumulation of matrix proteins in the extracellular space[50].

Decrease in the extravasation of blood was observed in the DOX+EPO group as compared to DOX-treated group. EPO has been linked to angiogenesis by enhancing proliferation and migration of endothelial cells[43]. EPO promotes an increase in the number of EPCs, their ability for tube formation, and capillary density. EPO also promotes neovascularization by directly mitogenic effects on endothelial cells and local upregulation of vascular endothelial growth factor (VEGF)[47].

In the current study, increase in CD34 immune expression between cardiac myocytes in the DOX-treated group was noticed. This mostly occur in response to release of certain molecules from ischemic tissue. It was proved that CD34 is expressed in tissue-resident mesenchymal stem cells (MSCs) that migrate to injured tissue sites that need repair. CD34+ cells are known for their high differentiation and proliferative capacities that play a critical role in the repair process[51,52]. However, combined administration of EPO with DOX caused a highly significant increase in the area percentage of positive CD34 immune reaction.

This indicates that EPO could efficiently enhance mobilization of stem cells from bone marrow and increase their homing to the injured cardiac tissue. Such findings coincide with that obtained by Oztas *et al*. (2020) who found that the safe use of EPO in diabetic rats may further increase tissue levels of CD34 and VEGF molecules, which are important for cellular regeneration and protection[25].

By two different mechanisms, CD34 cells could promote angiogenesis, neovascularization, and heart regeneration. First, by differentiating into endothelial cells and smooth muscle cells, which are the main structural elements of internal vascular walls, by this way CD34 cells can promote vascular re-endothelialization. Second, these cells play a substantial paracrine role in secreting substances that promote the growth of new blood vessels, inhibit the apoptosis of cardiomyocytes and endothelial cells, modify the extracellular matrix, and stimulate the activity of more progenitor cells[53].

CONCLUSION

DOX administration induces histological alterations in the cardiac muscle. EPO could protect the cardiac muscle against DOX effects by anti-apoptotic, anti-inflammatory and antioxidant mechanisms as well as via enhancing mobilization of stem cells to the injured tissues.

CONFLICT OF INTERESTS

There are no conflicts of interest.

REFERENCES

1. Abo Elfadl S, Shendi M, Reda A, Abdelhaleem A. Resveratrol pre-and post-treatment in doxorubicin-induced cardiac injury in relation to endogenous stem cell activation. Journal of Medical Histology. 2017; 1(1):19-29. https://dx.doi.org/10.21608/jmh.2017.1082.1017

2. Marinello J, Delcuratolo M, Capranico G. Anthracyclines as Topoisomerase II Poisons: From Early Studies to New Perspectives. Int J Mol Sci. 2018;19(11):3480. https://doi.org/10.3390/ijms19113480

3. Abushouk AI, Salem AMA, Saad A, Afifi AM, Afify AY, Afify H, Salem HSE, Ghanem E, Abdel-Daim MM. Mesenchymal Stem Cell Therapy for Doxorubicin-Induced Cardiomyopathy: Potential Mechanisms, Governing Factors, and Implications of the Heart Stem Cell Debate. Front Pharmacol. 2019;10:635. https://doi.org/10.3389/fphar.2019.00635
4. Rawat PS, Jaiswal A, Khurana A, Bhatti JS, Navik U. Doxorubicin-induced cardiotoxicity: An update on the molecular mechanism and novel therapeutic strategies for effective management. Biomed Pharmacother. 2021;139:111708. https://doi.org/10.1016/j.biopha.2021.111708
5. Shabaan DA, Mostafa N, El-Desoky MM, Arafat EA. Coenzyme Q10 protects against doxorubicin-induced cardiomyopathy via antioxidant and anti-apoptotic pathway. Tissue Barriers. 2021;2019504. https://doi.org/10.1080/21688370.2021.2019504
6. Kuşçu GC, Gürel Ç, Buhur A, Karabay Yavaşoğlu NÜ, Köse T, Yavaşoğlu A, Oltulu F. Fluvastatin alleviates doxorubicin-induced cardiac and renal toxicity in rats via regulation of oxidative stress, inflammation, and apoptosis associated genes expressions. Drug Chem Toxicol. 2022;1-12. https://doi.org/10.1080/01480545.2022.2043351
7. Brines M: Extrahematopoietic Actions of Erythropoietin. In: Singh AK, Williams GH (eds) Textbook of Nephro-Endocrinology. 2nd ed., Academic Press. London, UK. (2018)pp: 411-428. DOI: 10.4183/aeb.2017.523
8. J, Murguía-Castillo J, Marín-López AG, Gasca-Martínez Y, Cornelio-Martínez S, Beas-Zárate C. The Recombinant Human Erythropoietin Administered in Neonatal Rats After Excitotoxic Damage Induces Molecular Changes in the Hippocampus. Front Neurosci. 2019;13:118. https://doi.org/10.3389/fnins.2019.00118
9. Tóthová Z, Šemeláková M, Solárová Z, Tomc J, Debeljak N, Solár P. The Role of PI3K/AKT and MAPK Signaling Pathways in Erythropoietin Signalization. Int J Mol Sci. 2021;22(14):7682. https://doi.org/10.3390/ijms22147682
10. Poniewierska-Baran A, Rajewska-Majchrzak J, Ratajczak MZ. Erythropoietin enhances migration of human neuroblastoma cells: in *vitro* studies and potential therapeutic implications. J Cancer Stem Cell Res. 2017;5:e1003 PMCID: PMC5978773
11. Liu F, Wen Y, Kang J, Wei C, Wang M, Zheng Z, Peng J. Regulation of TLR4 expression mediates the attenuating effect of erythropoietin on inflammation and myocardial fibrosis in rat heart. Int J Mol Med. 2018;42(3):1436-1444. https://doi.org/10.3892/ijmm.2018.3707
12. Sidney LE, Branch MJ, Dunphy SE, Dua HS, Hopkinson A. Concise review: evidence for CD34 as a common marker for diverse progenitors. Stem cells. 2014;32(6):1380-1389. https://doi.org/10.1002/stem.1661
13. Prasad M, Corban MT, Henry TD, Dietz AB, Lerman LO, Lerman A. Promise of autologous CD34+ stem/progenitor cell therapy for treatment of cardiovascular disease. Cardiovasc Res. 2020;116(8):1424–1433. https://doi.org/10.1093/cvr/cvaa027
14. Koriem KM, Arbid MS. Role of caftaric acid in lead-associated nephrotoxicity in rats via antidiuretic, antioxidant and anti-apoptotic activities. J Complement Integr Med. 2018;15(2). https://doi.org/10.1515/jcim-2017-0024
15. Chen X, Guo Z, Wang P, Xu M. Erythropoietin modulates imbalance of matrix metalloproteinase-2 and tissue inhibitor of metalloproteinase-2 in doxorubicin-induced cardiotoxicity. Heart Lung Circ. 2014;23(8):772–777. https://doi.org/10.1016/j.hlc.2014.02.015
16. Pei Z, Hu J, Bai Q, Liu B, Cheng D, Liu H, Na R, Yu Q. Thymoquinone protects against cardiac damage from doxorubicin-induced heart failure in Sprague-Dawley rats. RSC Advances. 2018;8(26):14633-14639. https://doi.org/10.1039/c8ra00975a
17. Luo M, Chen PP, Yang L, Wang P, Lu YL, Shi FG, Gao Y, Xu SF, Gong QH, Xu RX, Deng J. Sodium ferulate inhibits myocardial hypertrophy induced by abdominal coarctation in rats: Involvement of cardiac PKC and MAPK signaling pathways. Biomed Pharmacother. 2019;112:108735. https://doi.org/10.1016/j.biopha.2019.108735
18. Bancroft JD, Layton C: The hematoxylins and eosin. In: Suvarna SK, Layton C, Bancroft JD (eds) Bancroft's theory and practice of histological techniques. 8th ed., Elsevier Churchill Livingstone. China, Edinburgh. (2019)pp: 126-138. https://doi.org/10.1016/C2015-0-00143-5
19. Bancroft JD, Layton C: Connective tissue and other mesenchymal tissues with their stains. In: Suvarna SK, Layton C, Bancroft JD (eds) Bancroft's theory and practice of histological techniques. 8th ed., Elsevier Churchill Livingstone. China, Edinburgh. (2019)pp: 135-175. https://doi.org/10.1016/C2015-0-00143-5
20. Magaki S, Hojat SA, Wei B, So A, Yong WH: An introduction to the performance of immunohistochemistry. In: Yong W. (eds) Biobanking. Methods in Molecular Biology, vol 1897. Humana Press. New York. (2019)pp: 289-298. https://doi.org/10.1007/978-1-4939-8935-5_25
21. Woods AE, Stirling JW: Transmission electron microscopy. In: Suvarna SK, Layton C, Bancroft JD (eds) Bancroft's theory and practice of histological techniques. 8th ed., Elsevier Churchill Livingstone. China, Edinburgh. (2019)pp: 434-475. https://doi.org/10.1016/C2015-0-00143-5

22. Hazra A, Gogtay N. Biostatistics Series Module 3: Comparing Groups: Numerical Variables. Indian J Dermatol. 2016;61(3):251-260. https://doi.org/10.4103/0019-5154.182416

23. Pajović V, Kovácsházi C, Kosić M, Vasić M, Đukić L, Brenner GB, Giricz Z, Bajić D, Ferdinandy P, Japundžić-Žigon N. Phenomapping for classification of doxorubicin-induced cardiomyopathy in rats. Toxicol Appl Pharmacol. 2021;423:115579. https://doi.org/10.1016/j.taap.2021.115579

24. Otter M, Csader S, Keiser M, Oswald S. Expression and Functional Contribution of Different Organic Cation Transporters to the Cellular Uptake of Doxorubicin into Human Breast Cancer and Cardiac Tissue. Int J Mol Sci. 2022;23(1):255. https://doi.org/10.3390/ijms23010255

25. Oztas ÝM, Meric M, Beyaz MO, Onalan MA, Sonmez K, Oter K, Ziyade S, Omer B, Alpagut U, Ugurlucan M. Cardioprotective effects of erythropoietin in diabetic rats determined by CD34 and vascular endothelial growth factor levels. Arch Med Sci Atheroscler Dis. 2020;5:e1-e12. https://doi.org/10.5114/amsad.2020.92346

26. Zhang X, Hu C, Kong CY, Song P, Wu HM, Xu SC, Yuan YP, Deng W, Ma ZG, Tang QZ. FNDC5 alleviates oxidative stress and cardiomyocyte apoptosis in doxorubicin-induced cardiotoxicity via activating AKT. Cell Death Differ. 2020;27(2):540-555. https://doi.org/10.1038/s41418-019-0372-z

27. Yao CX, Shi JC, Ma CX, Xiong CJ, Song YL, Zhang SF, Zhang SF, Zang MX, Xue LX. EGF Protects Cells Against Dox-Induced Growth Arrest Through Activating Cyclin D1 Expression. J Cell Biochem. 2015;116(8):1755-1765. https://doi.org/10.1002/jcb.25134

28. Goda AE, Elenany AM, Elsisi AE. Novel in *vivo* potential of trifluoperazine to ameliorate doxorubicin-induced cardiotoxicity involves suppression of NF-κB and apoptosis. Life Sci. 2021;283:119849. https://doi.org/10.1016/j.lfs.2021.119849

29. Abdo FKA, Ahmed FES, Shaheen MA, Mostafa SA. A comparative study of the Ameliorative effect of doxorubicin with vitamin E versus liposomal doxorubicin on the left ventricular histological and immunohisochemical changes induced by doxorubicin in adult male albino rats. Egyptian Journal of Histology. 2019;42(2):467-481. https://dx.doi.org/10.21608/ejh.2019.7015.1061

30. Rodrigues PG, Miranda-Silva D, Costa SM, Barros C, Hamdani N, Moura C, Mendes MJ, Sousa-Mendes C, Trindade F, Fontoura D, Vitorino R, Linke WA, Leite-Moreira AF, Falcão-Pires I. Early myocardial changes induced by doxorubicin in the nonfailing dilated ventricle. Am J Physiol Heart Circ Physiol.2019;316(3):H459-H475. https://doi.org/10.1152/ajpheart.00401.2018

31. Zhao L, Zhang B. Doxorubicin induces cardiotoxicity through upregulation of death receptors mediated apoptosis in cardiomyocytes. Sci Rep. 2017;7:44735. https://doi.org/10.1038/srep44735

32. Ye X, Li Y, Lv B, Qiu B, Zhang S, Peng H, Kong W, Tang C, Huang Y, Du J, Jin H. Endogenous Hydrogen Sulfide Persulfidates Caspase-3 at Cysteine 163 to Inhibit Doxorubicin-Induced Cardiomyocyte Apoptosis. Oxid med cell longev. 2022;2022:6153772. https://doi.org/10.1155/2022/6153772

33. Shati AA. Doxorubicin-induces NFAT/Fas/FasL cardiac apoptosis in rats through activation of calcineurin and P38 MAPK and inhibition of mTOR signalling pathways. Clin Exp Pharmacol Physiol. 2020;47(4):660-676. https://doi.org/10.1111/1440-1681.13225

34. Seke M, Petrovic D, Labudovic Borovic M, Borisev I, Novakovic M, Rakocevic Z, Djordjevic A. Fullerenol/iron nanocomposite diminishes doxorubicin-induced toxicity. J Nanopart Res. 2019;21:239. https://doi.org/10.1007/s11051-019-4681-4

35. Jin YZ, Gong YX, Liu Y, Xie DP, Ren CX, Lee SJ, Sun HN, Kwon T, Xu DY. Peroxiredoxin V Silencing Elevates Susceptibility to Doxorubicin-induced Cell Apoptosis via ROS-dependent Mitochondrial Dysfunction in AGS Gastric Cancer Cells. Anticancer Res. 2021;41(4):1831-1840. https://doi.org/10.21873/anticanres.14949

36. Yin J, Guo J, Zhang Q, Cui L, Zhang L, Zhang T, Zhao J, Li J, Middleton A, Carmichael PL, Peng S. Doxorubicin-induced mitophagy and mitochondrial damage is associated with dysregulation of the PINK1/parkin pathway. Toxicol In *Vitro*. 2018;51:1-10. https://doi.org/10.1016/j.tiv.2018.05.001

37. Sergazy S, Shulgau Z, Fedotovskikh G, Chulenbayeva L, Nurgozhina A, Nurgaziyev M, Krivyh E, Kamyshanskiy Y, Kushugulova A, Gulyayev A, Aljofan M. Cardioprotective effect of grape polyphenol extract against doxorubicin induced cardiotoxicity. Sci Rep. 2020;10(1):14720. https://doi.org/10.1038/s41598-020-71827-9

38. Yassien RI, Elsaid AF. The possible protective role of melatonin on doxorubicin induced cardiomyopathy of adult male albino rats. Egyptian Journal of Histology. 2017;40(1):25-36. https://dx.doi.org/10.21608/EJH.2017.3694

39. Siti HN, Jalil J, Asmadi AY, Kamisah Y. Effects of Quercetin on Cardiac Function in Pressure Overload and Postischemic Cardiac Injury in Rodents: a Systematic Review and Meta-Analysis. Cardiovasc Drugs Ther. 2020;36(1):15-29. https://doi.org/10.1007/s10557-020-07100-y

40. Ito Y, Yoshida M, Masuda H, Maeda D, Kudo-Asabe Y, Umakoshi M, Nanjo H, Goto A. Disorganization of intercalated discs in dilated cardiomyopathy. Sci Rep. 2021;11(1):1-13. https://doi.org/10.1038/s41598-021-90502-1

41. Li X, Pan F, He B, Fang C. Inhibition of ADAM10 ameliorates doxorubicin-induced cardiac remodeling by suppressing N-cadherin cleavage. Open Life Sci. 2021;16(1):856-866. https://doi.org/10.1515/biol-2021-0081

42. McNally EM, Mestroni L. Dilated Cardiomyopathy: Genetic Determinants and Mechanisms. Circ Res. 2017;121(7):731-748. https://doi.org/10.1161/CIRCRESAHA.116.309396

43. Haine L, Yegen CH, Marchant D, Richalet JP, Boncoeur E, Voituron N. Cytoprotective effects of erythropoietin: What about the lung?. Biomed Pharmacother. 2021;139:111547. https://doi.org/10.1016/j.biopha.2021.111547

44. Yousefian M, Hosseinzadeh H, Hayes AW, Hadizadeh F, Karimi G. The Protective Effect of Natural Compounds on Doxorubicin-Induced Cardiotoxicity via Nicotinamide Adenine Dinucleotide Phosphate Oxidase Inhibition. J Pharm Pharmacol. 2022;74(3):351-359. https://doi.org/10.1093/jpp/rgab109

45. Zhou Y, Su P, Pan Z, Liu D, Niu Y, Zhu W, Yao P, Song Y, Sun Y. Combination Therapy With Hyperbaric Oxygen and Erythropoietin Inhibits Neuronal Apoptosis and Improves Recovery in Rats With Spinal Cord Injury. Phys Ther. 2019;99(12):1679-1689. https://doi.org/10.1093/ptj/pzz125

46. Coimbra-Costa D, Garzón F, Alva N, Pinto TCC, Aguado F, Torrella JR, Carbonell T, Rama R. Intermittent Hypobaric Hypoxic Preconditioning Provides Neuroprotection by Increasing Antioxidant Activity, Erythropoietin Expression and Preventing Apoptosis and Astrogliosis in the Brain of Adult Rats Exposed to Acute Severe Hypoxia. Int J Mol Sci. 2021;22(10):5272. https://doi.org/10.3390/ijms22105272

47. Ammar HI, Saba S, Ammar RI, Elsayed LA, Ghaly WB, Dhingra S. Erythropoietin protects against doxorubicin-induced heart failure. Am J Physiol Heart Circ Physiol . 2011;301(6):H2413–H2421. https://doi.org/10.1152/ajpheart.01096.2010

48. He Q, Zhao X, Bi S, Cao Y. Pretreatment with Erythropoietin Attenuates Lung Ischemia/Reperfusion Injury via Toll-Like Receptor-4/Nuclear Factor-κB (TLR4/NF-κB) Pathway. Med Sci Monit . 2018;24:1251-1257. https://doi.org/10.12659/msm.905690

49. Lu J, Yao YY, Dai QM, Ma GS, Zhang SF, Cao L, Ren LQ, Liu NF. Erythropoietin attenuates cardiac dysfunction by increasing myocardial angiogenesis and inhibiting interstitial fibrosis in diabetic rats. Cardiovasc Diabetol. 2012;11:105. https://doi.org/10.1186/1475-2840-11-105

50. Wang LP, Yang XH, Wang XJ, Li SM, Sun N, Zhang T. Erythropoietin Decreases the Occurrence of Myocardial Fibrosis by Inhibiting the NADPH-ERK-NF-κB Pathway. Cardiology. 2016;133(2):97-108. https://doi.org/10.1159/000440995

51. Lin CS, Ning H, Lin G, Lue TF. Is CD34 truly a negative marker for mesenchymal stromal cells?. Cytotherapy. 2012;14(10):1159-1163. https://doi.org/10.3109/14653249.2012.729817

52. Oliveira MS, Carvalho JL, Campos AC, Gomes DA, de Goes AM, Melo MM. Doxorubicin has in *vivo* toxicological effects on ex *vivo* cultured mesenchymal stem cells. Toxicol Lett. 2014;224(3):380-386. https://doi.org/10.1016/j.toxlet.2013.11.023

53. Schneller D, Hofer-Warbinek R, Sturtzel C, Lipnik K, Gencelli B, Seltenhammer M, Wen M, Testori J, Bilban M, Borowski A, Windwarder M, Kapel SS, Besemfelder E, Cejka P, Habertheuer A, Schlechta B, Majdic O, Altmann F, Kocher A, Augustin HG, Luttmann W, Hofer E. Cytokine-Like 1 Is a Novel Proangiogenic Factor Secreted by and Mediating Functions of Endothelial Progenitor Cells. Circ res. 2019; 124(2):243-255. https://doi.org/10.1161/CIRCRESAHA.118.313645

الملخص العربى

يعزز الإريثروبويتين تحريك الخلايا الجذعية الذاتية CD٣٤+ ويمنع موت الخلايا المبرمج بوساطة كاسباس٣ في عضلة القلب للجرذان المعالجة بالدوكسوروبيسين: دراسة نسيجية

نورا حسن زيدان[١]، نوال عوض حسنين[١]، زينب عبدالحي صقارة[١]، وفاء سعد حامد[١]، أماني عبدالفتاح محمد عبدالفتاح[٢,٢]

[١]قسم الأنسجة الطبية وبيولوجيا الخلية، كلية الطب، جامعة المنصورة، المنصورة، مصر

[٢]قسم العلوم الطبية الأساسية، كلية الطب، جامعة الملك سلمان العالمية، جنوب سيناء، مصر

الخلفية: إن استخدام الدوكسوروبيسين كعقار مضاد للأورام محدود بسبب السمية القلبية. تم اقتراح الإريثروبويتين كعامل قوي لحماية القلب.

الهدف من البحث: هدفت هذه الدراسة إلى تقييم الدور الوقائي للإريثروبويتين في السمية القلبية التي يسببها الدوكسوروبيسين وكذلك دور الإريثروبويتين في تحريك الخلايا الجذعية المشتقة من نخاع العظام إلى الأنسجة المصابة.

مواد وطرق البحث: تم تقسيم اثنين وثلاثين من ذكور الجرذان البيضاء البالغة الذين تتراوح أوزانهم من ١٨٠ إلى ٢٠٠جرام إلى أربع مجموعات متساوية. المجموعة الضابطة (المجموعة١) تلقت محلولًا فسيولوجيًا ملحيًا (١مل/ كجم/ يوميًا). مجموعة الإريثروبويتين (المجموعة٢) تلقت إرثروبويتين بشري مؤتلف (٢٥٠٠وحدة دولية/ كجم، ٣مرات أسبوعيًا). المجموعة المعالجة بالدوكسوروبيسين (المجموعة٣) تلقت الدوكسوروبيسين (٢,٥مجم/ كجم، ٣مرات أسبوعيًا). مجموعة الدوكسوروبيسين+ الإريثروبويتين (المجموعة٤) تلقت الإريثروبويتين بالتزامن مع الدوكسوروبيسين و قد تم إعطاء جميع الأدوية عن طريق الحقن داخل الصفاق لمدة أسبوعين. تم تحضير عينات من البطين الأيسر لجميع الجرذان وصباغتها للدراسة بالمجهر الضوئي (الهيماتوكسيلين والإيوسين، ماسون ثلاثية الألوان، حمض الفوسفو-تنجستيك هيماتوكسيلين، بالإضافة إلى الصبغة هستوكيميائية مناعية كاسباس٣ و CD٣٤) وكذلك بالمجهر الإلكتروني النافذ.

النتائج: تسبب الدوكسوروبيسين في تغير ملحوظ في السمات النسيجية لألياف عضلة القلب بالإضافة إلى زيادة كبيرة في النسبة المئوية لمساحة الألياف الكولاجينية وكذلك زيادة في التعبير المناعي لكاسباس٣. أدى التعاطي المشترك للإرثروبويتين مع الدوكسوروبيسين إلى تحسن في السمات النسيجية لألياف عضلة القلب، وانخفاض كبير في النسبة المئوية لمساحة الألياف الكولاجينية وكذلك انخفاض في التعبير المناعي لكاسباس٣، وزيادة كبيرة في التعبير المناعي CD٣٤.

الاستنتاج: يقوم الإريثروبويتين بتأثيرات واقية قلبية على اعتلال عضلة القلب الناجم عن الدوكسوروبيسين عبر مسارات مضادة للموت المبرمج للخلايا ومضادة للتليف وكذلك عن طريق تحريك الخلايا الجذعية إلى الأنسجة المصابة.